

# Thoughts on a spin tune measurement and spin decoherence\*

W. W. MacKay, BNL, Upton, NY, USA Draft: March 5, 2006

## Abstract

In this paper, I study the feasibility of making a turn-by-turn spin measurement to extract the spin tune from a polarized beam injected perpendicular to the stable spin direction. For the ideal case of a zero-emittance beam with no spin-tune spread, there would be no spin decoherence and a measurement of the spin tune could easily be made by collecting turn-indexed polarization data of several million turns. However, in a real beam there is a momentum spread which provides a tune spread. With a coasting beam the tune spread will cause decoherence of the spins resulting in a fast depolarization of the beam in a thousand turns. With synchrotron oscillations the decoherence time can be greatly increased, so that a measurement becomes feasible with summation of the turn-by-turn data from a reasonable number of bunches ( $\lesssim 100$ ). Both the cases of a single Siberian snake and a pair of Siberian snakes are considered. By using spin tune measurements for both the single and double snake cases, we could vastly improve the calibration of the optimum settings for the RHIC snakes.

## INTRODUCTION

A pair Siberian snakes are used in each of the RHIC rings[1] to lock the spin tune at  $\frac{1}{2}$  and to maintain a vertical stable spin direction of the closed orbit. In order to study the decoherence of spins in RHIC, it is proposed to inject polarized protons into RHIC with polarization perpendicular to the stable spin direction. In principal, if the polarization could be measured from turn to turn, then for spin tunes near  $\frac{1}{2}$  we would see a spin flip every turn. Since the polarization asymmetries are small, an accurate measurement of polarization requires of order  $10^7$  events in the CNI polarimeter. On a single bunch crossing in RHIC the event rate at injection is more like one event every couple of bunch crossings, so the observation of the spin rotation will not be seen from turn to turn, but at least in some cases it should be observable in the FFT of the signal over thousands of turns. It only requires enough events to observe a definite signal in the FFT, rather than a precise value of polarization. The signal can be enhanced by adding data from multiple injections, since the injected polarization direction will always be the same on the first turn. In this paper I present preliminary simulations with a simple Monte Carlo event generator for the polarimeter and simple spin tracking in order to understand how to analyze such turn-by-turn polarization data.

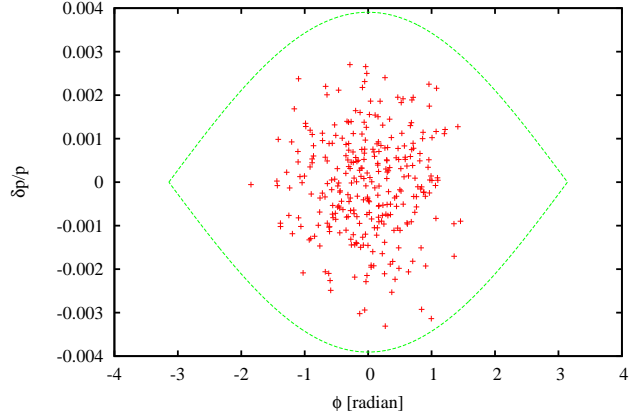


Figure 1: Typical initial Gaussian distribution of 300 particles in longitudinal phase space matched to the rf bucket. With 45 kV in each of the two accelerating cavities, the synchrotron frequency is about 23.5 Hz ( $Q_{sy} = 3 \times 10^{-4}$ ), and the rms momentum fraction and bunch lengths are respectively  $\sigma_p/p = 0.00116$  and  $\sigma_z = 1.01$  m.

The polarization of a bunch of  $N$  protons is defined as

$$\vec{P} = \frac{1}{N} \sum_{j=1}^N \frac{\vec{S}_j}{|S_j|} \quad (1)$$

where  $\vec{S}_j$  is the spin vector of the  $j^{\text{th}}$  proton and  $|S_j|$  is the magnitude of a single proton's spin vector. The unit vectors  $\hat{x}$ ,  $\hat{y}$ , and  $\hat{z}$  are respectively in the radial, vertical, and beam directions. The RHIC polarimeters are capable of measuring only both components of polarization in the transverse plane with projections vertical and radial projections  $P_y = \hat{y} \cdot \vec{P}$  and  $P_x = \hat{x} \cdot \vec{P}$ .

## SIMULATION OF POLARIZATION OSCILLATIONS

The decoherence of polarization was simulated by generating a Gaussian distribution in longitudinal phase of a number of particles, typically  $N = 300$  protons were generated, as shown in Fig. 1. The distribution was matched to the rf bucket with RHIC parameters with an rf voltage of  $V_{rf} = 90$  kV, harmonic number  $h = 360$ , transition gamma  $\gamma_t = 22.98$ , and ring circumference  $L = 3833.845$  m. All particles were assumed to have the same polarization at injection; however, a reduced factor of 50% polarization was later applied before generating events in the CNI polarimeter.

At fixed energy for the synchronous particle, the proton spins were tracked with energy oscillations, but no betatron

\* Work performed under the auspices of the U. S. DOE.

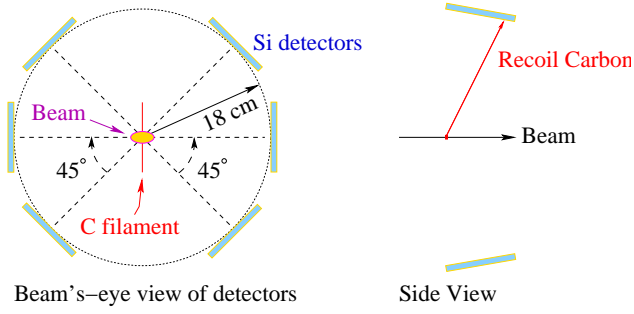


Figure 2: Layout of the six silicon detectors in the CNI polarimeter. The six detectors cover an azimuthal angle of about  $7.6^\circ$ .

oscillations; the distribution of particles was assumed to have zero transverse emittances. An average polarization for the distribution was calculated every turn. This average polarization was then projected onto the plane transverse to the beam direction at the polarimeter, and random events were generated and binned in azimuth into the six detectors (see Fig. 2) and written to a file every turn. Typically, it was assumed that on average there would be about one recoil carbon detected every two bunch crossings. The binned results for each turn were summed over multiple bunches to increase statistics.

## ONE SNAKE

For a flat ring with one snake, the spin tune  $\nu_s$  may be obtained from the one-turn spin rotation matrix. If we consider the Blue Ring of RHIC (see Fig. 3), the rotation matrix for a complete turn starting at the CNI polarimeter is

$$\mathbf{M} = \mathbf{R}_{\hat{y}}(G\gamma\theta_2) \mathbf{R}_{\hat{a}}(\mu) \mathbf{R}_{\hat{y}}(G\gamma\theta_1), \quad (2)$$

where  $\theta_1 + \theta_2 = 2\pi$  with  $\theta_1$  being the azimuthal location of the snake relative to the CNI polarimeter.

The snake's rotation axis is along along the unit vector

$$\hat{a} = \hat{z} \cos \phi + \hat{x} \sin \phi,$$

For the **bo3-snk7** and **bi9-snk7** snakes the angle  $\phi$  takes nominal values  $\pi/4$  and  $3\pi/4$ , respectively. The rotation matrix for a general left-handed rotation by an angle  $\alpha$  about a vector  $\hat{n}$  is given by

$$\mathbf{R}_{\hat{n}}(\alpha) = \mathbf{I} \cos(\alpha/2) + i(\hat{n} \cdot \vec{\sigma}) \sin(\alpha/2), \quad (3)$$

with the usual Pauli matrices

$$\sigma_x = \begin{pmatrix} 0 & 1 \\ 1 & 0 \end{pmatrix}, \sigma_y = \begin{pmatrix} 0 & -i \\ i & 0 \end{pmatrix}, \text{ and } \sigma_z = \begin{pmatrix} 1 & 0 \\ 0 & -1 \end{pmatrix}. \quad (4)$$

From the trace of the one-turn matrix, we get

$$\cos(\pi\nu_s) = \cos(G\gamma\pi) \cos(\mu/2), \quad (5)$$

for a snake rotation angle of  $\mu$ . If either  $G\gamma$  is equal to an integer plus  $1/2$  or  $\mu = 180^\circ$ , then the spin tune will be

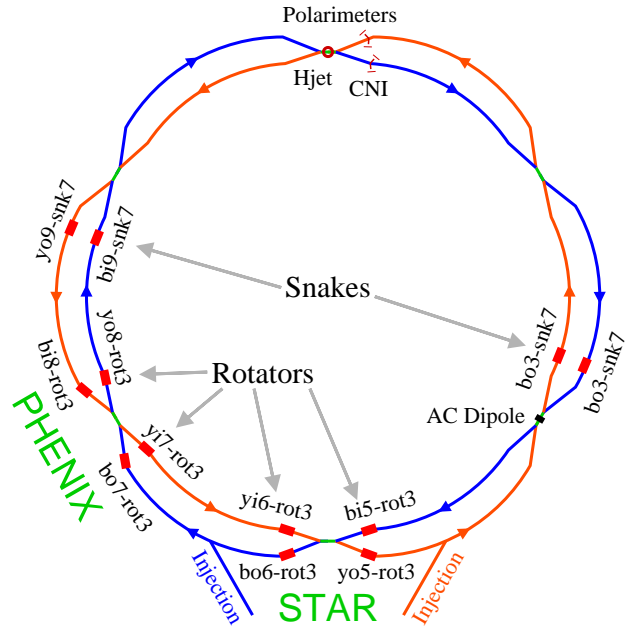


Figure 3: Layout of RHIC polarization elements.

exactly  $1/2$ . For small perturbations the spin tune deviation is

$$\delta\nu_s \simeq (-1)^{n+1} \frac{1}{2} \delta\Gamma \delta\mu, \quad (6)$$

where

$$\nu_s = \frac{1}{2} + \delta\nu_s, \quad (7)$$

$$G\gamma = n + \frac{1}{2} + \delta\Gamma, \quad (8)$$

$$\mu = \pi + \delta\mu \quad (9)$$

and  $n$  is an integer. Since a rotation of  $\pi + \delta\mu$  about a vector  $\hat{n}$  is equivalent to a rotation of  $\pi - \delta\mu$  about the vector  $-\hat{n}$ , the deviation of the spin tune from  $1/2$  could also have the opposite sign. Then more generally, near a half-integer tune we have

$$\delta\nu_s \simeq \pm \frac{1}{2} \delta\Gamma \delta\mu.$$

We should be able to set the extraction energy within 0.05 of 46.5 in units of  $G\gamma$ . I expect that the snake rotation angles in RHIC are within  $1^\circ$  of  $180^\circ$ .

By analogy with betatron oscillations, a spin chromaticity may be defined as

$$\xi_{sp} = p \frac{d\nu_s}{dp} = \beta^2 G\gamma \frac{d\nu_s}{d(G\gamma)}. \quad (10)$$

Figure 4 shows the variation of spin tune with one slightly detuned snake. At the half integer resonance, the spin chromaticity is largest, so we should expect the largest decoherence of spins perpendicular to the stable spin direction to appear when  $G\gamma$  is an integer plus a half.

At integer values of  $G\gamma$ , the chromaticity is zero. Having  $\xi_{sp} = 0$  at the imperfection resonances allows complete spin flipping of all the spins with a partial snake at integer



Figure 4: Spin tune for a flat ring with one snake detuned to  $\mu = 179.5^\circ$ . Near integer values of  $G\gamma$  the spin chromaticity  $\xi_{sp}$  approaches zero.

intrinsic resonances as in the AGS. The top plot of Fig. 5 shows decoherence of the spins without synchrotron oscillations for several values of  $G\gamma$ ; note the shortest decoherence time is at 46.5 with increasing decoherence times as  $G\gamma$  is increased towards 47.

With a momentum spread, the spins of different energies precess at different rates and tend to move apart, but as the energies oscillate, the energies of the lower and higher momenta particles become reversed so that the spins which have moved apart then move back towards each other. In the lower plot of Fig. 5 synchrotron oscillations are included so the spin coherence oscillates for  $G\gamma$  away from the integer, and at 46.5 the average decoherence time is much longer than without synchrotron oscillations. To make a quick estimate of the decoherence time in the number of turns, we can ask: how many turns does it take for a  $+1\sigma$  particle in the momentum distribution to advance  $180^\circ$  ahead of the synchronous particle? This gives a rough estimate of

$$\begin{aligned} N_{\text{decoh}} &\simeq \frac{1}{\pi \xi_{sp}(\sigma_p/p)} \\ &= \frac{1}{\pi \times 0.20 \times 0.00117} \simeq 1360 \text{ turns} \end{aligned} \quad (11)$$

when there are no synchrotron oscillations. With synchrotron oscillations the spins re-cohere after approximately one synchrotron period:

$$\frac{1}{Q_{sy}} \simeq \frac{1}{0.000299} = 3344 \text{ turns.} \quad (12)$$

Figure 6 shows the behavior of the tracking of Fig. 5 over a much longer period with synchrotron oscillations. After a while the oscillatory nature appears to have damped to a value of about 60% of the initial polarization. Figure 7 shows an FFT of the simulated polarimeter events corresponding to the tracking in Figure 6; with  $G\gamma = 46.5$ , the spin tune appears exactly at 0.5.

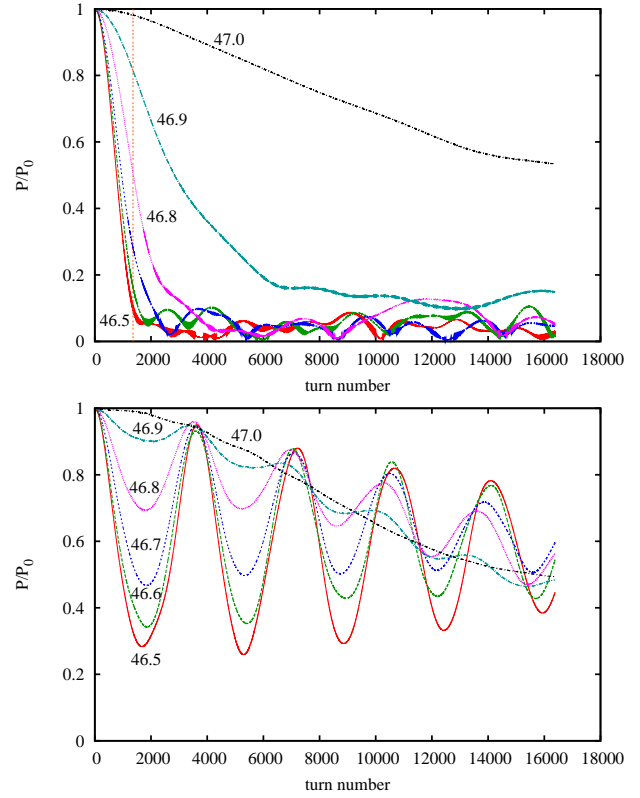


Figure 5: Simulated spin decoherence with for a bunch of 300 particles with longitudinal emittance 0.3 eVs. Curves of decreasing negative slopes from  $G\gamma = 46.5$  to 47 in steps of 0.1 are shown. The upper plot without synchrotron oscillations shows a rapid decrease in polarization, while the lower plot with synchrotron oscillations ( $V_{rf} = 90$  kV,  $Q_{sy} = 3 \times 10^{-4}$ ) shows longer coherences of an oscillatory nature for  $G\gamma$  away from integral values. In both cases, spins were tracked with the snake detuned to  $\mu = 179.5^\circ$ . The light vertical line in the upper plot indicates the decoherence estimate of  $N_{\text{decoh}} = 1360$  as described in the text.

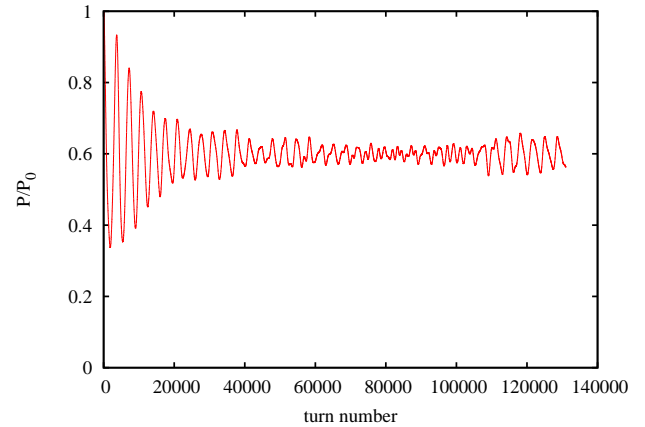


Figure 6: Total polarization with extended tracking of the parameters shown in the lower plot of Fig. 5.

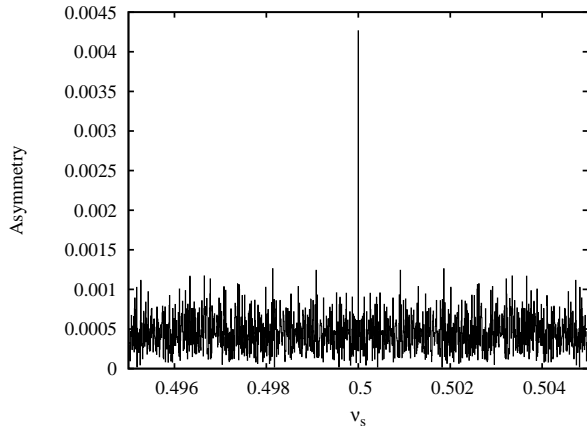


Figure 7: FFT amplitude of the simulated polarimeter asymmetry.  $\nu_s = 0.50000$ . Gaussian bunches of 300 particles with an rms emittance of 0.3 eVs were generated for  $G\gamma = 46.5$ , and the snake was detuned to a  $179.5^\circ$  rotation. The turn-by-turn results polarimeter from 30 bunches were accumulated assuming an initial polarization of 50% with a polarimeter asymmetry of 1%.

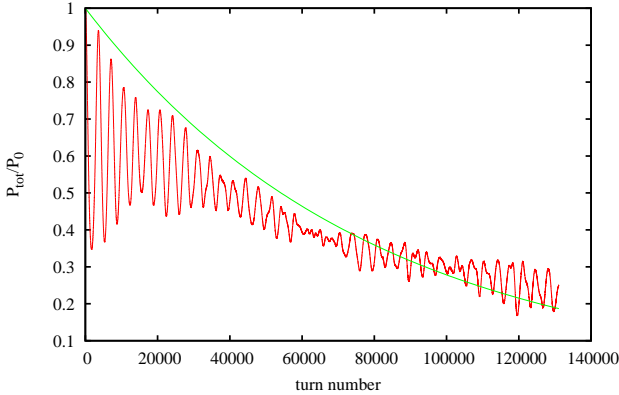


Figure 8: Simulation of total polarization with a shift of energy.  $Q_{sy} = 3 \times 10^{-4}$ . A Gaussian distribution of 300 particles with an rms emittance of 0.3 eVs was generated for  $G\gamma = 46.6$ , and the snake was detuned to a  $179.5^\circ$  rotation. An exponential curve is plotted for reference with a 1 s lifetime.

When the central energy is increased from  $G\gamma = 46.5$  to 46.6, the decoherence is stronger with the average polarization dropping well below the 60%-of-input value after  $10^5$  turns as shown in Fig. 8. A zoomed-in plot of the first 16000 turns (Fig. 9) also shows the vertical projection of polarization. Figure 10 shows the simulated spin tune ( $\nu_s = 0.49956$ ) obtained from an FFT of average polarization direction of 300 protons with a slightly detuned snake. Synchrotron sidebands are also visible. In the FFT of the corresponding simulated polarimeter data (shown in Fig. 11) the peak for the spin tune is still evident, but the synchrotron sidebands are too weak to be seen.

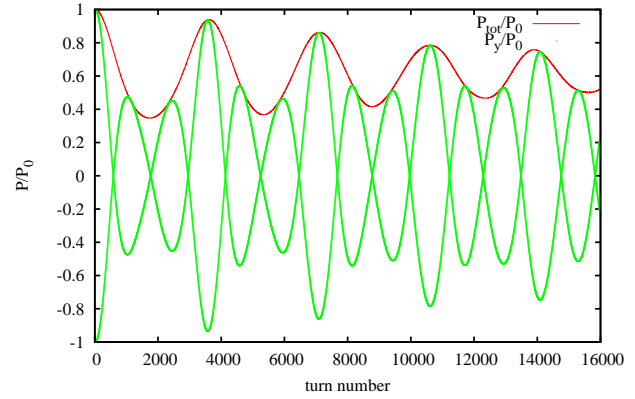


Figure 9: Total and vertical projection of the  $\vec{P}/P_0$  for the first 16000 turns. This is a zoomed-in plot of the first 16,000 turns of data plotted in Fig. 8.

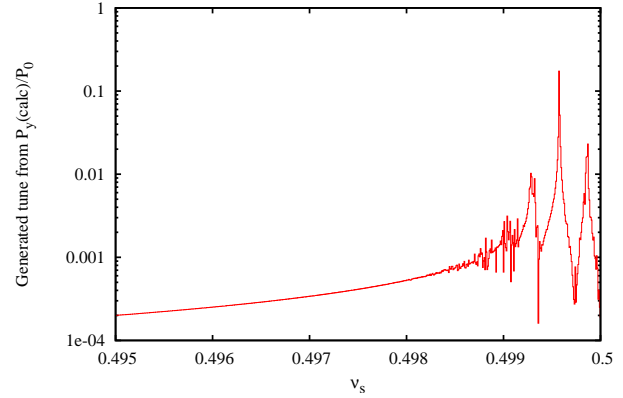


Figure 10: Spin tune with synchrotron sidebands with  $V_{rf} = 90$  kV, and  $Q_{sy} = 3 \times 10^{-4}$  for 300 particles generated with a longitudinal rms emittance of 0.5 eVs at  $G\gamma = 46.6$ . The snake was detuned to a  $179.5^\circ$  rotation.

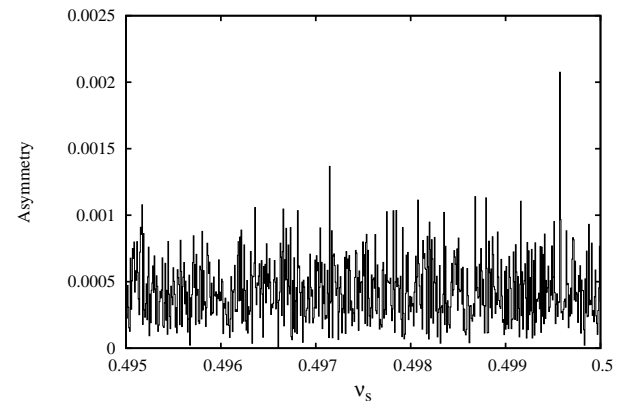


Figure 11: FFT amplitude of the simulated polarimeter asymmetry.  $\nu_s = 0.49956$ . Gaussian bunches of 300 particles with an rms emittance of 0.3 eVs was generated for  $G\gamma = 46.6$ , and the snake was detuned to a  $179.5^\circ$  rotation. The turn-by-turn results polarimeter from 30 bunches were accumulated assuming an initial polarization of 50% with a polarimeter asymmetry of 1%.

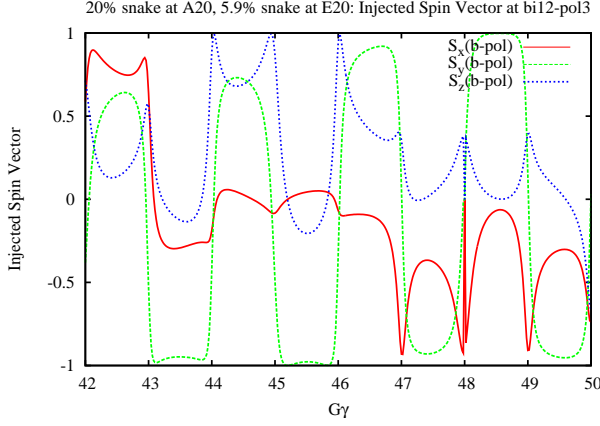


Figure 12: Injected polarization direction at CNI polarimeter in the first turn in the Blue Ring. At  $G\gamma = 46$ , the nominal injected spin direction is primarily longitudinal on the first turn.

## TWO SNAKES

With both full snakes in a RHIC ring, the stable spin direction at injection is vertical, so to measure decoherence, we would want to inject the bunches with horizontal polarization. By transferring the polarization from the AGS at an integer value of  $G\gamma$  rather than an integer plus a half, the spins will be primarily in the horizontal plane. Matching of the transfer of polarized protons from AGS to RHIC has been simulated at different energies to track the nominal polarization direction from the AGS onto the closed orbits of both RHIC rings right after the injection kickers[8]. Extending this to the first passage of the corresponding CNI polarimeter during the first turn, yields Fig. 12 for the Blue Ring and Fig. 13 for the Yellow Ring.

Since we would like to have a strong signal in the radial direction, particularly if the spin tune is very close to  $1/2$ , the chosen injection energy should have a large radial component of polarization on the first turn. Examining Figs. 12 and 13, the best energies closest to our normal operation would occur at  $G\gamma = 47$  in the Blue Ring and  $G\gamma = 46$  or  $47$  in the Yellow Ring. For the purpose of these simulations, I shall consider injection into the Yellow Ring at  $G\gamma = 46$ , with the polarization direction

$$\vec{P}_0(\text{CNI}) = \begin{pmatrix} -0.9936 \\ -0.0290 \\ -0.1090 \end{pmatrix}, \quad (13)$$

at the Yellow CNI Polarimeter on the first turn.

## SNAKE CALIBRATION

For a ring with a single snake, the spin tune may be obtained from

$$\cos(\pi\nu_s) = \cos(G\gamma\pi) \cos \frac{\mu}{2}, \quad (14)$$

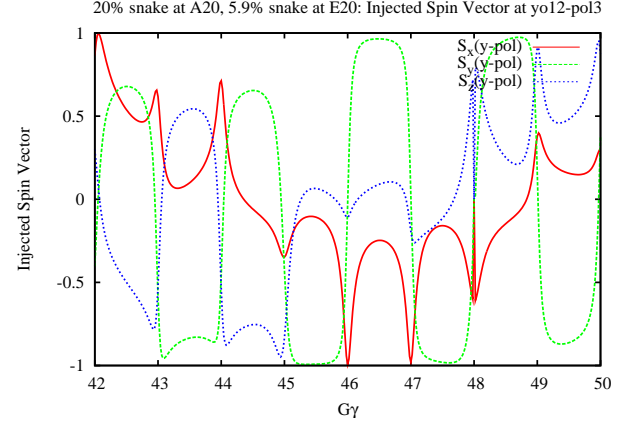


Figure 13: Injected polarization direction at CNI polarimeter in the first turn in the Yellow Ring. At  $G\gamma = 46$  the nominal injected spin direction is almost completely radial at the polarimeter on the first turn.

where  $\mu$  is the rotation angle of the snake. The spin tune is independent of the direction of the snake's rotation axis so long as the axis is in the horizontal plane. At integral values of  $G\gamma = n$ ,

$$\delta\nu \simeq (-1)^n \frac{\delta\mu}{\pi}, \quad (15)$$

where  $\mu = \pi + \delta\mu$  and  $\nu_s = 1/2 + \delta\nu$ .

For the two-snake case, the spin tune may be obtained from

$$\begin{aligned} \cos(\pi\nu_s) &= \cos(G\gamma\pi) \cos \frac{\mu_1}{2} \cos \frac{\mu_2}{2} \\ &\quad - \cos(\phi_1 - \phi_2) \sin \frac{\mu_1}{2} \sin \frac{\mu_2}{2}, \end{aligned} \quad (16)$$

where  $\mu_1$  and  $\mu_2$  are the rotation angles of the two snakes and  $\phi_1$  and  $\phi_2$  are the corresponding angles of the snake axes measured from the longitudinal  $z$ -axis in the horizontal plane. Assuming that both snakes were constructed identically, then with the same magnitude (but opposite sign) currents, we have

$$\mu = \mu_1 = -\mu_2, \quad (17)$$

$$\phi = \phi_1 = -\phi_2, \quad (18)$$

which simplifies Eq. 16 to

$$\cos(\pi\nu_s) = \cos(G\gamma\pi) \cos^2 \frac{\mu}{2} + \cos(2\phi) \sin^2 \frac{\mu}{2}. \quad (19)$$

For small deviations from nominal settings this gives

$$\delta\nu \simeq \cos(G\gamma\pi) \frac{(\delta\mu)^2}{4\pi} + \frac{2\delta\phi}{\pi}, \quad (20)$$

with  $\nu_s = 1/2 + \delta\nu$ ,  $\mu = \pi + \delta\mu$ , and  $\phi = \pi/4 + \delta\phi$ .

As an example, a simulation with synchrotron oscillations of almost 4.2 million turns ( $2^{22}$ ) at  $G\gamma = 45.95$  with the snakes detuned to have  $\mu_1 = \mu_2 = 179.5^\circ$ ,

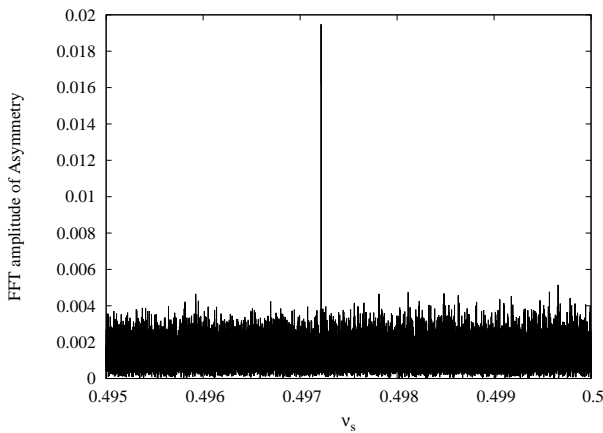


Figure 14: FFT amplitude of the spin tune signal from 30 bunches of 300 protons tracked for  $2^{22}$  turns. The parameters for this simulation were  $\delta\mu = -0.5^\circ$  and  $\delta\phi = 0.25^\circ$  for each snake,  $G\gamma = 45.95$ , and  $V_{rf} = 90$  kV. The resultant spin tune from the simulation was 0.4972162.

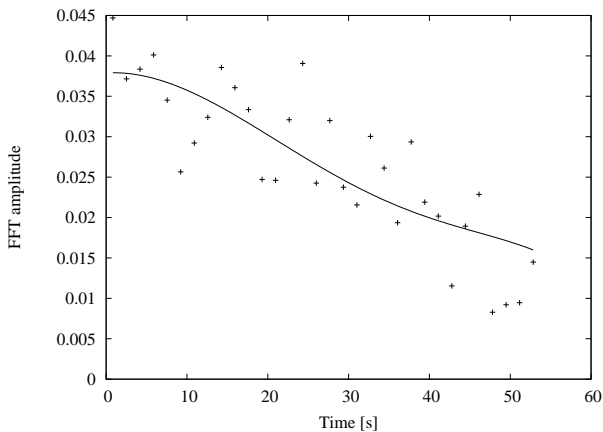


Figure 15: The data points are the FFT amplitudes calculated for the simulation of Fig. 14, but divided into 32 segments of  $2^{17}$  turns. The solid curve is the average polarization scaled to fit the FFT data. The scaling factor was fit to be  $0.0380 \pm 0.0013$ .

$\phi_1 = 44.75^\circ$ ,  $\phi_2 = 135.25^\circ$ . Summing the signal for 30 bunches yields a very strong signal in the spectrum from the simulated polarimeter data, as shown in Fig. 14. The solid curve in Fig. 15 shows a magnitude of tracked polarization scaled by a factor of 0.038. When the simulated polarimeter data for the 4.2 million turns is divided into 32 segments, the corresponding FFT amplitude of the peak bin shows a similar decoherence over time to the scaled polarization magnitude. The scale factor was determined from a least-squares fit of the curve to the points in Fig. 15.

So we see that the one-snake case is sensitive to the rotation angle of the snake  $\mu$ , whereas the two-snake case is more sensitive to the snake axis direction  $\phi$ . By combining measurements for both cases we should be able to improve

the snake calibration.

## CONCLUSIONS

This looks like it might actually work. Simulations of spin decoherence from energy spread combined with a Monte Carlo generator of the polarimeter signals show that the spin tune may be extracted from turn-tagged polarimeter data by using a standard FFT algorithm. Given that the signal does not decohere too quickly, it should be possible to extract the spin tune with extremely high precision using a modest number of bunches. Since these simulations only include synchrotron oscillations, SPINK will be used to do a more detailed tracking for the actual RHIC lattice with oscillations in all three planes.

Measurements of the spin tune with a single RHIC snake at injection at  $G\gamma = 45.5$  is sensitive to the snake rotation angle ( $\mu$ ). With two snakes at  $G\gamma = 46$ , the spin tune at injection is sensitive to the rotation axes ( $\phi$ ) of the two snakes, and rather insensitive to the snake rotation angles ( $\mu$ ). By combining measurements of the two cases, a much better calibration of the RHIC snakes should be possible.

## ACKNOWLEDGMENTS

The idea for this study originated in a discussion with Gerry Bunce one evening in the Main Control Room for the AGS and RHIC. The idea of turn-by-turn polarimeter measurements came from Mei Bai and Thomas Roser in connection with the possibility of spin-tune measurements by tilting the spin coherently with an ac dipole.

## REFERENCES

- [1] I. Alekseev et al., "Polarized proton collider at RHIC", *Nucl. Inst. and Meth.*, **A 499**, 392 (2003).
- [2] E. D. Courant, "Hybrid Helical Snakes and Rotators for RHIC", AGS/RHIC/SN No. 010, (1996).
- [3] V. Ptitsyn, "Symmetric Designs for Helical Spin Rotators at RHIC", AGS/RHIC/SN No. 005, (1996).
- [4] M. J. Syphers, "Spin Motion through Helical Dipole Magnets", AGS/RHIC/SN No. 020, (1996).
- [5] Mario Conte and William W. MacKay, *An Introduction to the Physics of Particle Accelerators*, World Sci., (1991).
- [6] William W. MacKay, *Supplementary Lecture Notes for Accelerator Physics*, (2005) (See Chapter 6.)  
URL: <http://www.rhichome.bnl.gov/People/waldo/lectures/supnotes.pdf>
- [7] E. D. Courant, "Computer Studies of Phase-Lock Acceleration" in *1961 Int. Conf. on High Energy Accelerators*, p. 201, Ed. M. H. Blewett, New York (1961).
- [8] W. W. MacKay, A. U. Luccio, and N. Tsoupras, "Spin Matching from AGS to RHIC with Two Partial Snakes", C-A/AP/? (200?).